Finite-difference time-domain modeling of transient infrasonic wavefields excited by volcanic explosions

K. Kim[1] and J. M. Lees[1]

Received 28 December 2010; revised 23 February 2011; accepted 2 March 2011; published 30 March 2011.

[1] Numerical modeling of waveform diffractions along the rim of a volcano vent shows high correlation to observed explosion signals at Karymsky Volcano, Kamchatka, Russia. The finite difference modeling assumed a gaussian source time function and an axisymmetric geometry. A clear demonstration of the significant distortion of infrasonic wavefronts was caused by diffraction at the vent rim edge. Data collected at Karymsky in 1997 and 1998 were compared to synthetic waveforms and variations of vent geometry were determined via grid search. Karymsky exhibited a wide range of variation in infrasonic waveforms, well explained by the diffraction, and modeled as changing vent geometry. Rim diffraction of volcanic infrasound is shown to be significant and must be accounted for when interpreting source physics from acoustic observations. **Citation:** Kim, K., and J. M. Lees (2011), Finite-difference time-domain modeling of transient infrasonic wavefields excited by volcanic explosions, *Geophys. Res. Lett.*, *38*, L06804, doi:10.1029/2010GL046615.

1. Introduction

[2] In the last 10 years infrasonic acoustic waves have played an increasingly important role in understanding vent dynamics during explosive activity at numerous volcanoes [*Garces and McNutt*, 1997; *Johnson et al.*, 2003; *Lees et al.*, 2004]. Relative to seismic recordings of volcanic explosions, infrasound has a simplified Green's function and can thus provide a direct measure of physical source dynamics in the vicinity of the volcanic vent. Signals in the infrasonic frequency band (<20 Hz) [*Wilson and Forbes*, 1969; *Kanamori et al.*, 1994] can have several sources, and explicit wave simulation is required to extract and separate source dynamics from propagation effects. Although infrasonic waves are not as affected by path effects at short source-receiver distances, the distorting effects of vent geometry and atmospheric perturbation must be considered and removed in order to understand the underlying source dynamics of individual explosions.

[3] We focus here on the volcanic vent geometry and its effect on infrasonic waveforms generated near the source during volcanic eruptions. When in close proximity to a volcano source (<10 Km) propagation paths can be approximated by straight lines and atmospheric refraction and reflection distortion are, for the most part, negligible [*Johnson et al.*, 2006; *Ripepe et al.*, 2007]. Here we model infrasound wavefields passing through a volcanic vent with varying radii and compare them with observations from Karymsky volcano, Russia. Wavefront deformation through the vent and past the rim is shown to be considerable and in significant agreement with field observations. We attribute the wave distortion to diffraction at the edge of the vent.

2. Data Acquisition

[4] Karymsky Volcano is a 1540-m andesitic cone located in the central portion of Kamchatka's main active arc in Russia. Seismo-acoustic data presented here were collected at Karymsky volcano during two field surveys in August 1997 and September 1998 [*Johnson et al.*, 2003; *Lees et al.*, 2004]. In 1997 and 1998, Karymsky exhibited long periods of discrete Strombolian explosive activity with a repetitive explosions ranging from 5 to 20 events per hour, on average. Stations were instrumented with PASSCAL Reftek A-07 and A-08 dataloggers with 3-component broadband seismometers and microphones on the lower flanks of the volcano, at distances 1500–5000 m from the summit crater (Figure 1a). In 1998, a microphone equipped with the Larsen-Davis 2570 electret condenser was used with laboratory-calibrated single-pole corner frequency at 0.27 Hz (3 dB down) and nominal sensitivity of 48 mV/Pa [*Johnson*, 2007]. In 1997, however, a different electret condenser-based microphone was deployed [*Johnson et al.*, 2003; *Ripepe et al.*, 2007]. The 1997 microphone was found to be sensitive to changes in pressure rather than absolute pressure, so measures of the time-derivative of pressure are recorded in the field. The electret condenser microphone has a flat response function in the audible band (20 Hz–20 KHz), however calibration and sensitivity below 20 Hz is unavailable at this time, so detailed deconvolution is not possible. Since the signal-to-noise ratio for both 1997 and 1998 data are high and observations are in such good agreement with synthetic modeling, we present results from the 1997 modeling as corroboration of our approach in spite of the lack of calibration.

[5] Among thousands of events recorded, 214 explosions (134 from 1997 and 80 from 1998) were selected for comparison to synthetic wave propagation modeling. Criteria for selection included: (1) impulsive, short duration signals (<10 s) and (2) high signal-to-noise ratio (28 ± 9 dB) below 10 Hz. We thus avoid signals whose waveforms potentially interact with conduit walls and the fluid/air interface.

3. FDTD Propagation Model

[6] A Finite-Difference Time-Domain (FDTD) method was used to synthesize acoustic wave propagation formulated as a set of first-order, velocity-pressure coupled differential equations [*Ostashev et al.*, 2005]. FDTD methods are powerful numerical tools widely used to study wave propagation in heterogeneous media including the atmosphere

[1]Department of Geological Sciences, University of North Carolina at Chapel Hill, Chapel Hill, North Carolina, USA.

0094-8276/11/2010GL046615

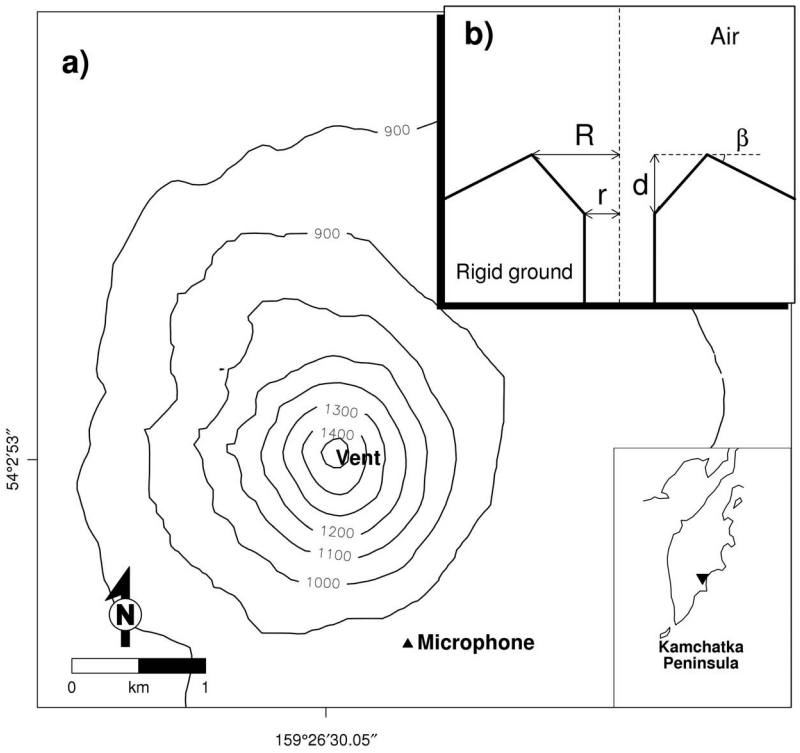

Figure 1. (a) Map of Karymsky volcano showing the microphone position during the two field experiments. (b) Cross-sectional view of the modeling domain illustrating the parameters and geometry of the model. Values of the parameters are listed in Table 1.

and the ground [*de Groot-Hedlin*, 2008]. To approximate the derivatives in the acoustic wave equation with finite differences, a staggered difference algorithm [*Yee*, 1966] was used in a two-dimensional cylindrical spatial domain. Time marching was staggered between the computations of pressure and particle velocity in the time domain. By restricting the computation to an axisymmetric cylindrical representation (volcanic cone and vent) calculations can be performed quickly on a desktop computer.

[7] The perfectly matched layer technique [*Berenger*, 1994; *Liu*, 1999] was adapted for absorbing boundary conditions achieving highly effective suppression of reflections at the domain boundaries. In order to examine effects of ground surface and topographic reflections, diffractions, and scattering by the volcano geometry, a rigid boundary condition between the air and solid surface was implemented via the method of images [*Morse and Ingard*, 1986]. Intrinsic attenuation and moving media are ignored in this simulation. In order to reduce numerical errors arising from the "staircase" representation of the rigid boundary, the model is spatially discretized using 20 grid points per wavelength, double the recommended minimum of 10 [*Wang*, 1996].

[8] The volcanic conduit was modeled as an air-filled cylinder buried in a rigid volcanic cone, where the atmosphere was treated as a fluid halfspace connected to the magmatic system through the open vent (Figure 1b). In real volcanic environments, the conduit is likely filled with multi-phase fluids consisting of air, gas, and magma. In this study we simply assume that the top of the conduit consists of constant 340 m/s velocity air. Inhomogeneities and wind in the atmosphere, nonlinear behavior, and the effects of gravity are ignored. Supersonic flux of the initial mass and very large pressure perturbations ($>10^3$ Pa) can cause nonlinear shock waves. Strombolian ejection velocities, however, generally range up to a few hundred meters per second [*Sparks*, 1997]. Source pressures calculated from Karymsky data do not exceed 10^2 Pa, using point source assumptions [*Johnson*, 2003], so we have adopted the linearized acoustic equation. Because our aim is to investigate deformation of wavefronts passing through the vent, longitudinal reflection at the air-magma interface is suppressed by incorporating an absorbing boundary at this interface, preventing downgoing waves from being reflected back towards the summit.

[9] The average outer radius of the active crater remained mostly constant at 45 meters from 1996 to 1998 based on geodetic observations (A. Ozerov, personal communication, 2010). Inner vent radius, depth and source frequency were allowed to vary as model parameters (Table 1).

[10] The direct source of volcanic infrasound is atmospheric vibration at the air-magma interface. This pertur-

Table 1. Modeling Parameters Illustrated in Figure 1b

Parameters	Values
Acoustic velocity for air	340 m/s
Density for air	1 kg/m^3
Source-time duration (T)	0.1 s–2 s
Radius of vent (r)	1 m–45 m
Depth of crater (d)	0 m–80 m
Radius of crater (R)	45 m
Slope of volcanic flank (β)	30°

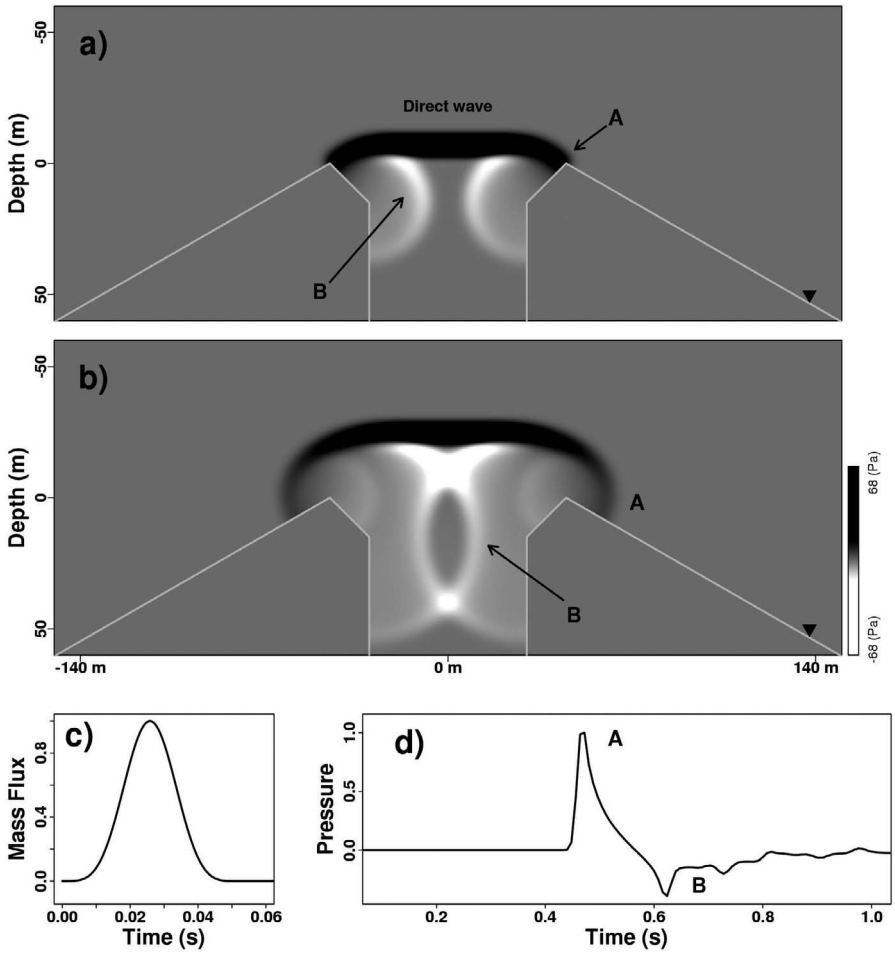

Figure 2. Modeling results that illustrate diffraction effects at the edge of the vent. The mass flux and pressure are normalized to the maximum value. (a) Snapshot of wavefronts diffracted from inner vent corner. Two edge waves with opposite polarities are indicated at A (positive) and B (negative). (b) Snapshot showing diffraction from outer crater rim. (c) Blackman-Harris function which has a 3dB cutoff frequency at 1/(time duration) Hz. (d) Synthetic acoustogram recorded at the receiver (inverted triangle in Figure 1a). Peaks of the two edge waves (A and B) are clearly evident.

bation can be generated by mass outflux through, or accelerating movement of, the interface. We use mass outflux here as the source because we have observed, visually, gas emission associated with infrasonic events. High amplitude infrasound is more effectively excited by explosive gas emission than by large displacement of the air-magma interface [*Johnson et al.*, 2004]. Mass flux is assumed here to be spatially constant over the air-magma interface, exciting only the plane wave mode in the conduit. The plane wave condition is not exact, as real volcanic sources most probably simultaneously excite radial modes. The conduit walls act as waveguides, however, preventing the low frequency radial modes from being generated. Therefore, the plane wave is the predominant mode in the conduit as long as the vent radial dimension is smaller than the source wavelength. A gaussian-shaped pulse (Blackman-Harris window function) was used as the source-time-function for the mass flux (Figure 2c).

4. Results

[11] We first present modeling results from a vent with varying radii to compare with analytic solutions and to provide insight into diffraction effects at the edge of the vent. Sound propagation excited by a vibrating piston buried in the rigid halfspace has been widely studied in the field of acoustics [*Harris*, 1981]. Briefly, acoustic wavefronts of overpressure from a vibrating piston are composed of two components: a plane "direct wave" generated by vertical piston movement propagating along the conduit axis, followed by spherical, "edge waves", produced by diffraction along the vent edge (Figure 2a). In the cylindrical region immediately above the vent, the consequent wavefront consists of a direct wave followed by edge waves. Outside the cylindrical region, however, two edge waves with opposite polarities are the major contributors to the wavefield [*Weight and Hayman*, 1978].

[12] In most exploding volcano situations, for reasons of safety, receivers are restricted to flanks away from the vent rim, and edge effects contribute considerably to observed signals. If the source is impulsive (Figure 2c), the two inverted pulses are readily observed on real recordings (Figure 2d). The lag and amplitudes of the two inverted pulses are constrained by the conduit radius, assuming the radius is constant with depth. In our modeling domain, however, acoustic waves are affected by diffraction from

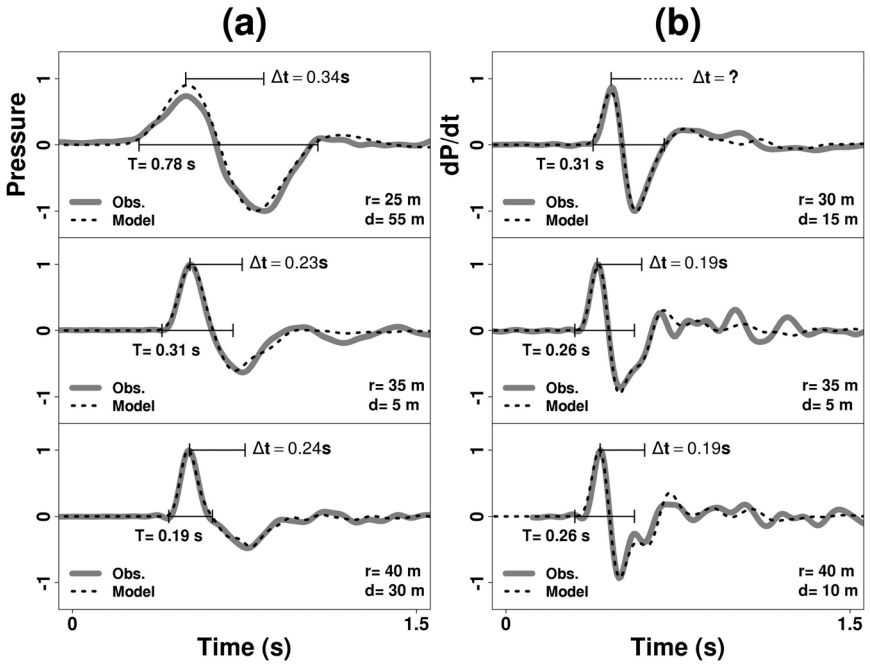

Figure 3. Comparison between model results and observations from Karymsky. The synthetic and observed signals are filtered by a low-pass filter (~10 Hz) and normalized to the maximum value. Modeling parameters are presented for each figure, where T = source-time duration, r = radius of inner vent and d = depth of crater, Δt = time lag between two inverted pulses attributed to overlapping of edge waves. (a) Synthetic waves are modeled by gaussian source-time functions with different durations listed on the figure. Accompanying observations are from the 1998 experiments. (b) Comparison between synthetic waveforms and 1997 observations, where the rate of change of overpressure was modeled. (top) The latter arriving edge wave is indistinguishable from the first because they overlap smoothly.

the edge of the inner and outer apertures of the crater. In Figures 2a and 2b, two diffractions are illustrated. When the original waves emanate from the inner vent, they diffract and the diffracted waves oscillate horizontally inside the crater, generating multiple reflected waves. Thus, where the vent radius increases, the original waves are distorted in a complex way governed by both inner and outer vent radii and the associated crater depth.

[13] Figure 3 shows a series of transient acoustic waveforms deformed by different geometries and different source-time-functions. The waveform distortion from the two edge waves with opposite polarities is clear, and sensitive to the geometry of the vent. These synthetic waveforms were compared to real data observed at Karymsky and the fit is extremely good (>0.83 cross-correlation values for 90% of events). One series of observations which illustrate the waveform dependency on the vent geometry and the source time duration is illustrated in Figure 3. Impulsive explosions and subsequent oscillations were successfully reproduced by numerical modeling. Numerical modeling indicates that diffraction at the vent edge plays a significant role in the observed waveforms.

5. Discussion and Conclusion

[14] Based on the theory of acoustic radiation from a vibrating piston, the contribution of diffracted edge waves to the wavefield depends on the vibration velocity and the diameter of the piston. If the wavelength of the vibration is much larger than the piston diameter, the larger of the two edge waves overlaps such that the radiating pressure waves are proportional to the time derivative of the vibration velocity, i.e., the acceleration. In this limit, the piston corresponds to a point source radiator. On the other hand, if the velocity wavelength is shorter than the piston diameter, two edge waves can be resolved without overlap. In this case, each edge wave closely resembles (slightly dispersed) the vibration velocity rather than the acceleration [*Weight and Hayman*, 1978]. Infrasound data recorded in the field at Karymsky exhibit this diffraction phenomenon. When the source wave length (265 m) is larger than the outer crater diameter (90 m), the observed waveform reduces to the time derivative of the source function (Figure 3a, top). The duration of the pressure perturbation is almost the same as that of the source time function representing mass flux. When the source wavelength (64 m) is shorter than the crater, however, the two edge waves can be separated such that the first arrived edge wave is highly correlated to the mass flux function (Figure 3a, bottom). The latter edge wave is more attenuated and may be contaminated by reverberations within the crater. This dependency on vent dimensions and source wavelength was observed also in 1997 (Figure 3b) where the instrument recorded the time-derivative pressure field [*Ripepe et al.*, 2007].

[15] The assumption of a gaussian shaped source function and plane waves appears to be justified by the excellent correlation of model results with field observations. First, because only short duration pulses were selected from the Karymsky data, sources must be simple. Second, the vent wall behaves as a waveguide and the plane wave dominates

even though the source wavelength is slightly shorter than or equal to the vent diameter. Third, the real source may have a vertical component amplitude larger than the radial component. The true directivity of the source can not be estimated without observations of the direct wave (as defined previously) above the vent or refracted in the far field.

[16] We focused here primarily on the presence of edge waves near a volcanic crater and on how they are related to source waveforms. A more detailed study may provide insight to the relation of the time lag (Δt) between edge waves and the vent geometry, although that is beyond the scope of this paper. The time lag has a strong dependence on the source waveform and vent geometry, however, if the pulse wavelength is shorter than the vent diameter (Figure 3a, bottom), the two edge waves do not overlap and the time lag can be reduced to a function of geometric parameters alone. In the case of a simple piston with constant radius, this time lag corresponds only to the piston diameter [*Weight and Hayman*, 1978]. However, in our model with varying radii, the time lag depends on the inner vent radius and the depth as well as the outer crater radius. High frequency pulses thus play a critical role for delineating detailed geometric features of the vent.

[17] FDTD modelings of infrasonic observations from Karymsky volcano showed that the wavefields in the near field are significantly affected by diffraction. The morphology of the crater plays an essential role in waveform distortion. Our results show that it is critical to take diffraction effects into account when interpreting source physics of volcanic explosions from acoustic observations.

[18] **Acknowledgments.** We thank to Maurizio Ripepe for advice on microphones and to Alexei Ozerov for providing geometric information. This project was funded by the National Science Foundation (grant EAR-0738768).

References

Berenger, J. (1994), A perfectly matched layer for the absorption of electromagnetic waves, *J. Comput. Phys.*, *114*(2), 185–200, doi:10.1006/jcph.1994.1159.

de Groot-Hedlin, C. (2008), Finite-difference time-domain synthesis of infrasound propagation through an absorbing atmosphere, *J. Acoust. Soc. Am.*, *124*(3), 1430–1441, doi:10.1121/1.2959736.

Garces, M. A., and S. R. McNutt (1997), Theory of the airborne sound field generated in a resonant magma conduit, *J. Volcanol. Geotherm. Res.*, *78*(3–4), 155–178, doi:10.1016/S0377-0273(97)00018-8.

Harris, G. (1981), Review of transient field theory for a baffled planar piston, *J. Acoust. Soc. Am.*, *70*(1), 10–20.

Johnson, J. B. (2003), Generation and propagation of infrasonic airwaves from volcanic explosions, *J. Volcanol. Geotherm. Res.*, *121*(1–2), 1–14, doi:10.1016/S0377-0273(02)00408-0.

Johnson, J. B. (2007), On the relation between infrasound, seismicity, and small pyroclastic explosions at Karymsky volcano, *J. Geophys. Res.*, *112*, B08203, doi:10.1029/2006JB004654.

Johnson, J. B., R. Aster, M. Ruiz, S. Malone, P. McChesney, J. Lees, and P. Kyle (2003), Interpretation and utility of infrasonic records from erupting volcanoes, *J. Volcanol. Geotherm. Res.*, *121*(1–2), 15–63, doi:10.1016/S0377-0273(02)00409-2.

Johnson, J. B., R. C. Aster, and P. R. Kyle (2004), Volcanic eruptions observed with infrasound, *Geophys. Res. Lett.*, *31*, L14604, doi:10.1029/2004GL020020.

Johnson, J. B., J. M. Lees, and H. Yepes (2006), Volcanic eruptions, lightning, and a waterfall: Differentiating the menagerie of infrasound in the Ecuadorian jungle, *Geophys. Res. Lett.*, *33*, L06308, doi:10.1029/2005GL025515.

Kanamori, H., J. Mori, and D. G. Harkrider (1994), Excitation of atmospheric oscillations by volcanic eruptions, *J. Geophys. Res.*, *99*(B11), 21,947–21,961, doi:10.1029/94JB01475.

Lees, J., E. Gordeev, and M. Ripepe (2004), Explosions and periodic tremor at Karymsky volcano, Kamchatka, Russia, *Geophys. J. Int.*, *158*(3), 1151–1167, doi:10.1111/j.1365-246X.2004.02239.x.

Liu, Q. (1999), Perfectly matched layers for elastic waves in cylindrical and spherical coordinates, *J. Acoust. Soc. Am.*, *105*(4), 2075–2084, doi:10.1121/1.426812.

Morse, P., and K. Ingard (1986), *Theoretical Acoustics*, 927 pp., Princeton Univ Press, Princeton, N. J.

Ostashev, V., D. Wilson, L. Liu, D. Aldridge, N. Symons, and D. Marlin (2005), Equations for finite-difference, time-domain simulation of sound propagation in moving inhomogeneous media and numerical implementation, *J. Acoust. Soc. Am.*, *117*(2), 503–517, doi:10.1121/1.1841531.

Ripepe, M., E. Marchetti, and G. Ulivieri (2007), Infrasonic monitoring at Stromboli volcano during the 2003 effusive eruption: Insights on the explosive and degassing process of an open conduit system, *J. Geophys. Res.*, *112*, B09207,doi:10.1029/2006JB004613.

Sparks, R. S. J. (1997), *Volcanic Plumes*, 574 pp., Wiley, New York.

Wang, S. (1996), Finite-difference time-domain approach to underwater acoustic scattering problems, *J. Acoust. Soc. Am.*, *99*(4), 1924–1931, doi:10.1121/1.415375.

Weight, J. P., and A. J. Hayman (1978), Observations of the propagation of very short ultrasonic pulses and their reflection by small targets, *J. Acoust. Soc. Am.*, *63*(2), 396–404, doi:10.1121/1.381730.

Wilson, C. R., and R. B. Forbes (1969), Infrasonic waves from Alaskan volcanic eruptions, *J. Geophys. Res.*, *74*(18), 4511–4522, doi:10.1029/JC074i018p04511.

Yee, K. (1966), Numerical solution of initial boundary value problems involving Maxwell's equations in isotropic media, *IEEE Trans. Antennas Propag.*, *14*(3), 302–307, doi:10.1109/TAP.1966.1138693.

K. Kim and J. M. Lees, Department of Geological Sciences, University of North Carolina at Chapel Hill, 104 South Rd., Mitchell Hall, CB #3315, Chapel Hill, NC 27599, USA. (keehoon@email.unc.edu; jonathan.lees@unc.edu)